Geofísica Internacional (2024) **63-4**: 1193 - 1207

Integrated geophysical characterization of Owu Gold mineralization part of Kushaka-Kusheriki Schist Belt, Northcentral Nigeria

Cyril C. Okpoli*[1], Oladele Olaniyan[2], Anthony V. Oyeshomo[1] and Promise Chidi[1]

Abstract

Integrated geophysical and geological surveys were used to characterize the gold mineralization at Owu, partof the Kushaka-Kusheriki schist belt in North Central Nigeria. Previous studies concentrated on geology and geochemical studies with no emphasis on the use of integrated studies and state-of-the-art tools aimed at characterizing gold mineralization. Detailed geological mapping was carried out to determine the various rock types and their structural framework. The geophysical surveys were carried out using the Proton Precession magnetometer and GDD 500 Time Domain Electromagnetic (TDEM) equipment to delineate their degree of magnetic susceptibility and induced polarization and dataset was enhanced using Fast Fourier Transforms (FFT).The geological survey showed the different rock types within the area and the geophysical survey produced the image of the subsurface and near surface structures. The datasets were subjected to different forms of filtering using Oasis Montaj software, thereby delineating the trend and target areas of proved gold mineralization. Geologically, the study area consists of phyllite, mica schist, amphibole schist, phyllitic schist, biotite schist exposed in a schist shear zone. Regional NE-SW foliated and folded axes of quartz veins intruded the gold mineralized bodies. Structurally, granitic intrusions are observed in the NE-SW direction, parallel to the regional foliation of the rocks. The total magnetic intensity, the vertical derivatives, horizontal gradient and analytical signal images revealed the high and low magnetic areas, and indicated the structures and lineaments to be trending in the NE–SW direction. Time domain Induced Polarization delineated the east-west direction major fault zones. The chargeability areas are due to high conductivity which trends, in the NE–SW direction suggesting the presence of gold and other heavy metals. The area of low chargeability is resistive and could represent the quartz veins in the area.

Key words: Gold, Magnetic intensity, chargeability, resistivity, shear zones.

Resumen

Se realizaron estudios geofísicos y geológicos integrados para caracterizar la mineralización de oro en Owu, parte del cinturón de esquisto de Kushaka-Kusheriki, en el centro norte de Nigeria. Investigaciones previas se concentraron en estudios geológicos y geoquímicos sin énfasis en el uso de métodos integrados y herramientas de última generación destinados a caracterizar la mineralización de oro. Se llevó a cabo un mapeo geológico detallado para determinar los distintos tipos de rocas y su estructura estructural. Los estudios geofísicos se llevaron a cabo utilizando el magnetómetro de precesión de protones y el equipo electromagnético de dominio de tiempo (TDEM) GDD 500 para delinear su grado de susceptibilidad magnética y polarización inducida y el conjunto de datos se mejoró mediante transformadas rápidas de Fourier (FFT). El estudio geológico mostró las diferentes tipos de roca dentro del área y el estudio geofísico produjo la imagen del subsuelo y las estructuras cercanas a la superficie. Los conjuntos de datos se sometieron a diferentes formas de filtrado utilizando el software Oasis Montaj, delineando así la tendencia y las áreas objetivo de mineralización de oro probada. Geológicamente, el área de estudio consiste en esquistos de filita, esquistos de mica, esquistos anfíboles, esquistos filiticos y esquistos de biotita expuestos en una zona de corte de esquistos. Ejes regionales NE-SW foliados y plegados de vetas de cuarzo invadieron los cuerpos mineralizados de oro. Estructuralmente se observan intrusiones graníticas en dirección NE-SW, paralelas a la foliación regional de las rocas. La intensidad magnética total, las derivadas verticales, el gradiente horizontal y las imágenes de señales analíticas revelaron las áreas magnéticas altas y bajas, e indicaron las estructuras y lineamientos con tendencia en la dirección NE-SW. La polarización inducida en el dominio del tiempo delineó las principales zonas de falla en dirección este-oeste. Las áreas de cargabilidad se deben a la alta conductividad que tiende en dirección NE-SW, lo que sugiere la presencia de oro y otros metales pesados. El área de baja cargabilidad es resistiva y podría representar las vetas de cuarzo de la zona.

Palabras clave: Oro, Intensidad magnética, cargabilidad, resistividad, zonas de corte.

Received: July 18, 2023; Accepted: January 10, 2024; Published on-line: October 1, 2024.

Editorial responsibility: Dr. Oscar C. Valdiviezo-Mijangos

* Corresponding author: Cyril C. Okpoli. E-mail: cyril.okpoli@aaua.edu.ng
[1] Department of Earth Sciences, Faculty of Science, Adekunle Ajasin University, PMB 1, Akungba-Akoko, Ondo State, Nigeria.
[2] Geodel integrated, Abuja, Nigeria

https://doi.org/10.22201/igeof.2954436xe.2024.63.2.1781

1. Introduction

In Nigeria, gold mineralization is often associated with quartz veins and other sulphide minerals mainly formed from hydrothermal fluid. Gold also occur in placer deposits of unconsolidated sand, sandstone and conglomerate. Primary mineralization is the accumulation of minerals in-situ. The bigger/wider the intrusion the better/higher the alteration. Gold mineralization in alteration zones and quartz veins is mostly associated with pyrite, chalcopyrite etc.

Cost-effective integrated geophysical techniques using magnetic survey and Time Domain Induced Polarisation (TDIP) were employed to understand geological structures. Application of several geophysical methods, such as simultaneous IP and resistivity aided in delineating prospective sites and enhanced interpretation of observed data. The magnetic and TDEM were used in prospective areas where outcrop is poor, or areas that have been subject to intense mineral search over a long period of time. Detailed mapping of the Kusheriki schist belt was carried out by Truswell and Cope (1963) and extended southwards to the Zungeru area by Ajibade (1988). Four formations were recognized for the Kusheriki Schist Group, namely: 1. The Kusheriki Psammite Formation at the base of the succession, 2. The Kushaka Schist Formation, 3. The Zungeru Granulite Formation and 4. The Birnin Gwari Schist Formation at the top.

Gold occurs in primary hydrothermal veins, as volcanic and alluvial deposits in association with pyrite, chalcopyrite, arsenopyrite, pyrrhotite, sylvanite, krennerite, calaverite, altaite, tetradymite, scheelite, ankerite, tourmaline, quartz (Hilson, 2006).

The focus of this study is to characterize gold mineralization in the study area using geological and integrated geophysical methods (magnetic and time domain induced polarization, as mentioned above) To identify and map-out geological units and structures that are geologically prospective, define areas for further investigation and drill targets of the primary gold host; areas of economic alluvial deposits and other economic mineralization within the study area.

1.1 Previous studies

The occurence of gold in Nigeria is generally in veins and placers around southwestern and northwestern schist belts. Examples of mineralized schist belts in Nigeria are: Iperindo, Maru, Anka, Kwaga, Gurmana, Birnin-yauri, Okolum and Dogon-Daji. They are associated with the regional NE-SW and NNE-SSW fault systems. Some of the most important occurrences are at Maru, Anka, Kwaga, Gurmana, Birnin-yauri, Okolum, Dogon-Daji and Iperindo areas, all associated with the schist belts (Okpoli *et al.* 2022). The gold veins are hosted by various rock types ranging from gneisses, schists, phyllites and quartzites to amphibolites and aureoles of granitic intrusions. The regional and local controls are mainly structural, made up of a system of transcurrent and subsidiary faults and other structures of Pan African age (Ho and Groves, 1987). According to Ekwueme and Matheis (1995), the structural dynamics serve as conveyor of hydrothermal fluids and the interactions with lineaments/ rock walls favors deposition of gold. The regional fault systems related to the Pan African crustal sutures (Kerrich and Wyman, 1990) are characteristic of mesothermal gold deposit worldwide. Spatial regional structural architectures are associated to mesothermal gold deposits (Kuster, 1990, Maurin, and Lancelot, 1990). The spatial relationship with transcrustal lineaments is a probable indication that the gold deposits are products of convergent margin tectonics (McCurry and Wright, 1977, McDonald, 1986,). The association of the lineaments with magmatic bodies couple with their extensive length (>100 km) implying transcrustal lineaments that extends to the lower crust and mantle (Maurin and Lancelot, 1990). Thus, Nigerian Pan-African gold mineralisations are structurally controlled.

The different gold metallogenic provinces in Nigeria include: Maru gold mines; several abandoned mines in Kwali, Kuba, Jameson and Zuzzurfa associated with schists, Phyllites and quartzites in Anka and their veins are < 500m which strikes concordantly to the rock foliation. Malele NNE-SSW gold mineralised veins within the biotite-gneiss and chlorite; Kwaga and Tsofon Birnin Gwari mineralised gold; Zuru brittle gold-sulphide-carbonate quartz veins in Bin Yauri, hosted by intruded phyllites and tourmalinites to granodiorite; southern Kushaka, Gurmana- mineralised gold-quartz-sulphide veins/ stocks within gneiss and amphibolite rocks; Egbe-Isanlu >3 km NS-NNE mineralised gold-quartz in Okolom-Dogondaji hosted by schists, gneisses and amphibolites (Kinniard, 1984) and abandoned Iperindo mineralised gold-quartz-carbonate mine in Ifewara- Ilesha shear zone, southwestern Nigeria. They are hosted by biotite gneiss and mica schist (Hilson, 2006, Haruna, 2017).

2. Study area setting

The study area is located at Owu, Niger State North-Central Nigeria (6.7093°E9.8714°N) (Figure 1). The different rock types seen within the study area include, Phyllite/Phyllitic Schist, Schist/Amphibolite Schist, Granite Gneiss and Quartz trending NE-SW (Fitches *et al.*, 1985).

The soil type is formed from by-products of Precambrian Basement Complex rocks and sedimentary rocks. The vegetation like others in that region is of Sudan-Savannah vegetation and the climate is warm with temperature ranging from 24 °C to 36 °C.

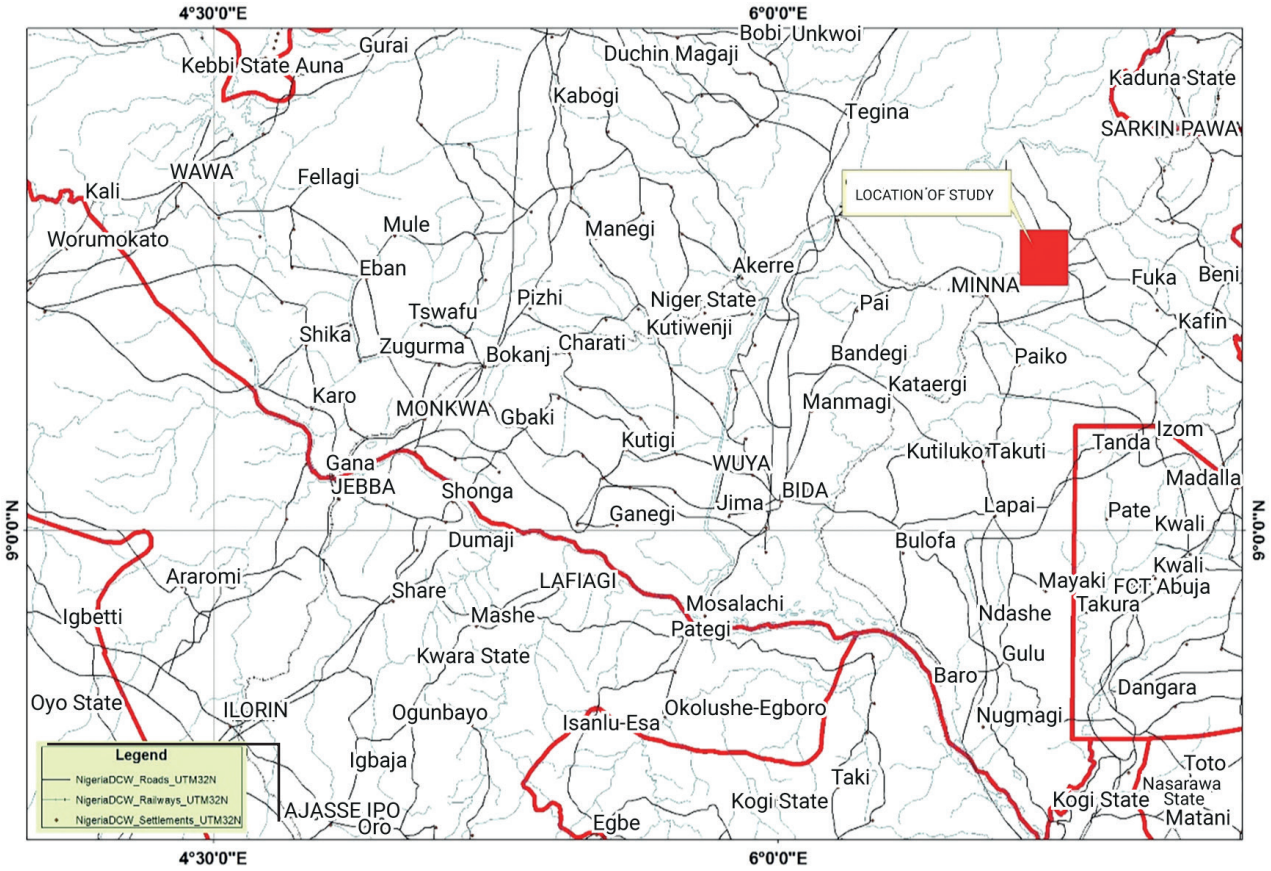

Figure 1. Administrative Map of Nigeria.

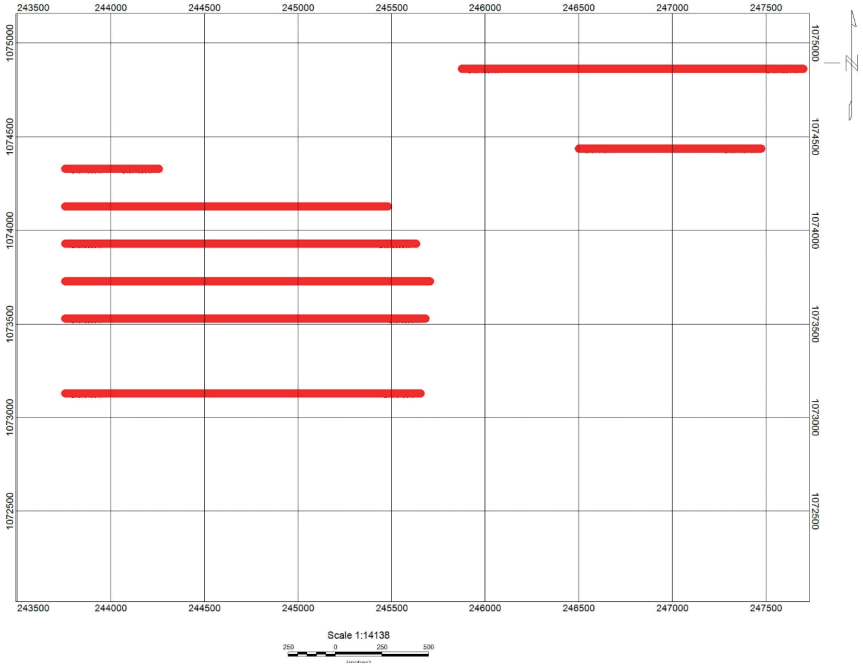

Figure 2. Profile line of IP survey map.

The area is surrounded by mountains and relatively flat, but the topography undulates gently with some valleys and floodplains. High elevated outcrops are not dominant in the area (Figure 3).

The study area lies in the Northcentral Nigeria and is made up of the migmatite-gneiss complex, Older granite and Schist belts. The isochron ages of this rocks ranges from Liberian to Pan-African. Examples are migmatite-gneiss, amphibolites,-quartzites, pelitic and calcareous rocks (metasediments). The Kusheriki schist belt group, which comprises of Kusheriki Psammite, Kushaka schist, Zungeru granulite and Birnin Gwari schist Formations overlying the metamorphosed Basement Complex of Nigeria. Elueze, 1981 reported that the study area that is demarcated by synclinal and anticlinal gneiss and characterised by numerous schist belt: semi-pelitic biotite-muscovite schist (garnet and staurolite), graphitic schists, phyllites and meta-siltstones, interbedded garnet grunerite iron Formation,diverse amphiboles with amphibolites, epidote-chlorite-talc-bearing schists associated with tholeiitic basalt. The rocks are estimated to be Kibaran (1,159± 70 Ma) in age (Kinniard, 1984).

3. Materials and methods

3.1 Geophysical Survey

Magnetic Survey and Induced Polarization methods were employed to study the area.

3.1.1 Magnetic Survey

Magnetic survey was used to search and delineate mineral bearing ore bodies, sedimentary structures and buried structures. Ground magnetic surveys were conducted with a Proton Precession magnetometer in grid formats covering the survey area. The acquired total magnetic data was corrected and downloaded into the survey database for quality control and checks. Profile data plotting and preliminary gridding was done using minimum curvature method at a cell size of 25m to assess noise in the data. Dropouts and spikes were later filtered from the data on a daily basis. At the end of the 124 km line survey, the merged magnetic data were micro levelled to remove directional noises along and across the survey line and the data were contoured using Oasis montaj software.

3.1.2 Induced Polarization (IP)

Time-domain induced polarization use the voltage decay as a function of time after an injected electric current is put off. IP identified economic minerals such as Gold, Lead/Zinc in the study area. The occurrence of primary gold and other sulphide mineralization was observed to be disseminated within the vein quartz and quarzitic material. Time Domain Induced Polarization (TDIP) survey was conducted across the interpreted magnetic structures and geochemical hotspots (Figure 2). Time domain, IP data were collected along the east-west profiles using a GDD 5000-watt transmitter and a 16-channel receiver (Figure 3). The

Figure 3. The GDD 500 set – up in the field.

setup utilized dipole-dipole array, conductor cables, two steel current electrodes and eight non-polarizable copper sulphate electrode pots (the receivers) spaced 50m apart, and with a 25m station interval over a 1.2 km distance. The survey protocols were done by injection of 2 seconds on and 2 seconds off duty cycle currents into the ground via a 5000-watt transmitter (Tx), while the receiver measures the decay of the primary voltage. Thirty readings were stacked to improve the signal/noise ratio.

4. Results and discussion

4.1 Ground Magnetic Survey

4.1.2. Total magnetic intensity

The total magnetic intensity map demonstrated the differences in character of high and low magnetic intensities and regional magnetic zones with most of them trending northeast – southwest direction. The magnetic zone division was based on the intensity, shape and pattern in magnetic signatures (Ademila *et al.*, 2019; Gunn *et al.*, 1997; Okpoli & Akinbulejo.2021; Okpoli *et al.*2022). Besides analytical signal that shows areas with high magnetic susceptibility as high anomalies, the TMI map shows high magnetic, intermediate and low magnetic susceptibility zones. The (blue to pink colored) are zones of low to high magnetic susceptibility zones respectively. Areas with the high magnetic susceptibility are observed to be within the sheared zone as seen in Figure 4 bounded all-round by intermediate magnetic susceptible Metasediments and granitic intrusions. The northern part and pockets of southern part of the TMI map shows the high magnetic susceptible Basement Complex.

4.1.3 The First Vertical Derivative

The first vertical derivative map (Figure 5) highlights rock contacts, faults, veins and other lineaments in both NE and NW directions. The lineaments (faults) are well pronounced in the NE-SW and NW-SE directions showing high magnetic intensity due to the gold mineralization hosted in that direction. Also, the trends are evidence of pronounced episodes of orogeny that occurred in this schist belt.

4.1.4. Second Vertical Derivative

The second derivative filter attenuate broad and more regional anomalies, enhancing the local magnetic responses and emphasizing the plan view edges and extents of target zones (especially intra-basement anomaly sources). Prominent magnetic lineaments are observed and marked by the red lines as shown in figure 6. The target gold anomaly magnetic lineaments are de-

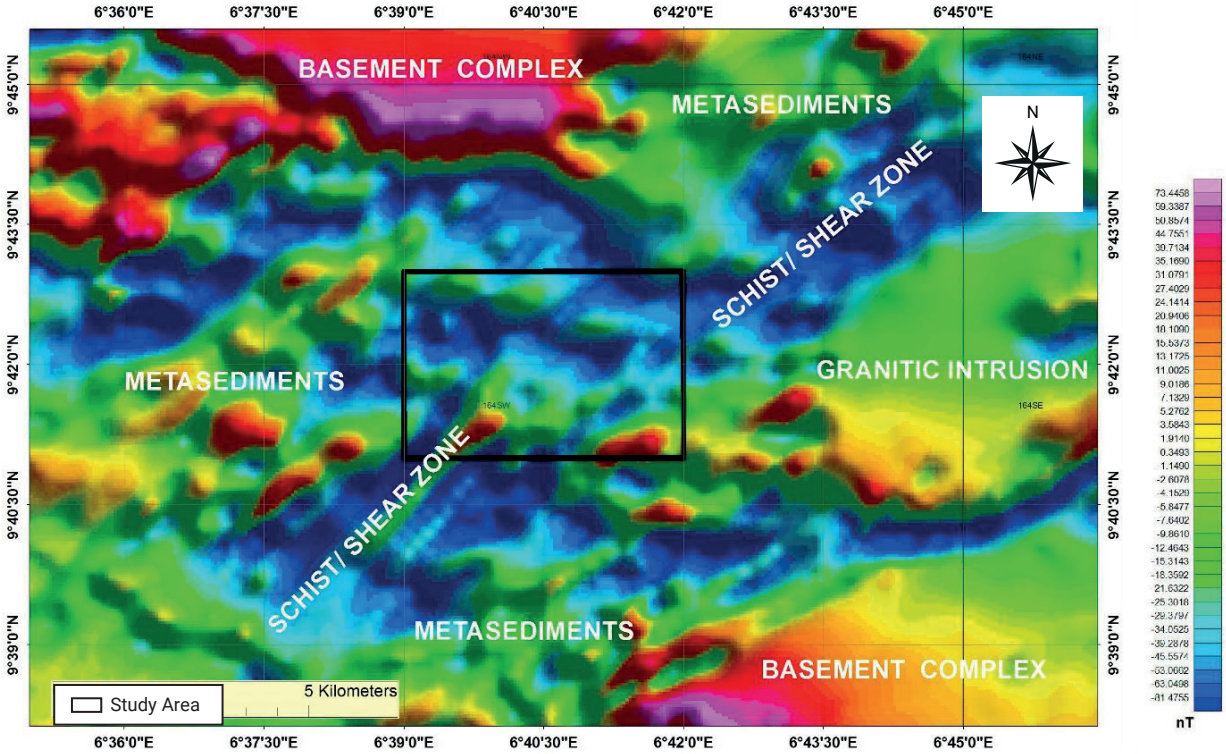

Figure 4. Total Magnetic Intensity map.

Table 1. Detail geological mapping of the study area

Location Id	Longitude (E)			Latitude (N)			Elevation (M)	Lithology	Colour	Texture
L1	6	40	29.7	9	40	59.9	322	Phyllitic Schist	Grey- Light Grey	Fine-Medium
L1b	6	40	29.7	9	40	59.9	322	Quartz Body/ Rubbles	Brownish	Medium-Coarse
L2	6	40	19	9	41	51.4	340	Schist	Grey- Light Grey	Fine-Medium
L3	6	40	11.3	9	41	11.3	363	Schist	Grey-Dark Grey	Fine-Medium
L3b	6	40	7	9	41	46.6	368	Quartz Rubbles	Brown-Reddish	Medium-Coarse
L3c	6	40	3.6	9	41	45.7	352	Biotite Schist	Dark-Grey	Fine-Medium
L4	6	40	3.4	9	41	42.4	361	Phyllitic Schist	Dark-Light Grey	Fine-Medium
L5	6	39	42.6	9	41	38	334	Schist	Dark-Grey	Fine-Medium
L5b	6	39	40	9	41	33.6	322	Schist	Dark-Grey	Fine-Medium
L6	6	39	18.3	9	41	31.2	335	Granite-Gneiss	Greyish	Medium
L7	6	39	15	9	41	38.3	320	Schist	Light-Grey	Fine-Medium
L8	6	39	51.4	9	42	18.2	321	Amphibole Schist/ Gneiss	Greenish/Light& Dark Band	Fine-Medium
L9	6	41	36.2	9	42	53.2	368	Schist		Fine-Medium
L9b	6	41	34.5	9	42	52.1	371	Phyllite	Light-Grey	Fine-Medium
L10	6	41	37.2	9	42	57.2	367	Phyllite	Light-Grey	Medium-Coarse
L11	6	41	30	9	42	53	365	Phyllite	Brownish- Grey	Fine-Medium
L12	6	41	48.8	9	42	38.2	353	Quartz Body/Veins	Whitish/Milky	Fine-Medium
L13	6	41	41.7	9	42	25.2	359	Quartz Rubbles	Whitish/Milky	Fine
L14	6	41	51.6	9	42	19.8	356	Quartz Body	Whitish/Milky	Fine
L15	6	41	35.7	9	42	15.5	357	Quartz Body	Whitish/Milky	Fine
L16	6	41	30.8	9	42	7.7	328	Phyllitic Schist	Light-Grey	Fine-Medium
L17	6	41	27.7	9	41	50.3	320	Phyllitic Schist	Grey-Dark	Fine-Medium
L18	6	41	14.6	9	41	59	328	Phyllitic Schist	Grey-Light Grey	Fine-Medium
L19	6	41	6.6	9	41	53.4	340	Quartz Body	Whitish/Milky	Fine
L20	6	40	32.4	9	42	0	325	Phyllitic Schist	Grey	Fine-Medium
L21	6	40	41.4	9	42	13.7	331	Phyllite	Grey	Fine
L22	6	41	23.2	9	42	46.6	355	Granite-Gneiss	Light-Grey	Medium-Coarse
L22b	6	41	28.6	9	42	51.2	357	Granite-Gneiss	Dark-Grey	Medium-Coarse
L23	6	41	31.9	9	42	52.7	364	Schist	Grey	Medium-Coarse
L24	6	42	0	9	41	24	331	Phyllitic Schist	Grey	Fine
L25	6	41	51.5	9	41	27	335	Quartz Veins	Reddish-Brown	Fine-Medium
L26	6	41	15.2	9	41	28.1	338	Quartz Rubbles	Reddish-Brown	Fine-Medium
L26b	6	41	4.3	9	41	29	332	Quartz Rubbles	Whitish/Milky	Fine
L27	6	41	15.3	9	41	15.6	327	Phyllitic Schist	Grey-Light Grey	Fine-Medium
L28	6	41	28	9	41	10	326	Phyllite	Grey	Fine-Medium
L29	6	40	35.9	9	42	34.8	311	Quartz Rubbles	Whitish-Brownish	Fine-Medium
L30	6	40	23	9	41	31.8	329	Amphibole Schist	Greenish-Grey	Fine-Medium
L31	6	40	14.8	9	41	28.8	319	Amphibole Schist	Greenish-Grey	Fine-Medium
L32	6	40	4.3	9	41	9.1	313			
L33	6	40	6.9	9	41	16.1	318	Quartz Rubbles	Whitish-Brownish	Fine-Medium
L33b	6	40	8.2	9	41	17.1	318			
L34	6	40	8.6	9	41	18	317	Schist	Grey	Fine-Medium

Table 2. List of structural data acquired on the study area.

Location id	Strike	Dip/direction	Observation
L1	16	53/E	Parralle sets of quartz veins embedded within the rock
L1b			An altered quartz body at 7-m eastward of location 1
L2			Highly weathered exposure
L3	10	82/E	Hilly exposure trending n-s with quartz veins & rubbles
L3b			The dimension of the quartz rubbles is about 20m by 10m
L3c			
L4	5	59/E	A thin quartz veins embedded within the rock and q/r
L5	40	64/E	Quartz veins observed & lots of quartz rubbles
L5b	22	66/E	Quartz veins with strike of 19 & thickness of 16cm
L6	38	59/E	It occurs in bouldery form with lots of quartz veins
L7	12	E	Stream sediment are being packed for gold panning
L8	51	40/E(se)	Two lithologies(amphibole schist & gneiss) & quartz r.
L9	166	E	Signs of mineralization on quartz rubbles
L9b	188	82/E	Quartz veins in concordant with the country rock
L10	28	50/W	Quartz veins of about 12cm thick and veinlet(1cmby10cm)
L11	9	48/E	Upland bouldery exposure with lots quartz vein
L12	42		Parralle sets of quartz veins with a width of about 60m
L13			A gentle uphill of quartz rubbles
L14	22	46/E	Bouldery exposure of quartz body of about(50mby30m)
L15	128		Upland of quartz body in insitu & quartz rubbles
L16	38	68/E	The exposure is highly foliated with some quartz veins
L17	38	68/E	The exposre is dipping eastward & trending ne-sw
L18	11	40/E	Quartz veins of about 10cm by 50cm & some thin veinlet
L19			An upland exposure quartz body in bouldery form
L20	180		The exposure is along a stream channels
L21	10	68/W	A highly jointed exposure with a lots of quartz veins
L22	19		Hilly exposure wth several boulders & thin quartz veins
L22b	20		The exposure has a quartz veins & a lots of quartz r.
L23	22		A contact btw the schist & granite gneiss
L24	32	28/E	It occurs along a stream & it's becoming gradational
L25	140		An occurrence of quartz veins with sign of alteration
L26			A hilly exposure of quartz rubbles
L26b			A fixed spread of quartz rubbles of about 150m
L27	54	26/E	A flat exposure that is highly weathered
L28	54	32/E	A very small exposure
L29			A spread of quartz rubble on gentle upland
L30			A small flat exposure
L31	20	41/E	A well foliated body along a stream channel with q.R
L32			The pit is about 5m deep with no traceable vein
L33			Quartz rubbles close to a first order stream
L33b			First order stream running south to river mauna/ose
L34	4	70/E	Quartz veins embedded within the host rock

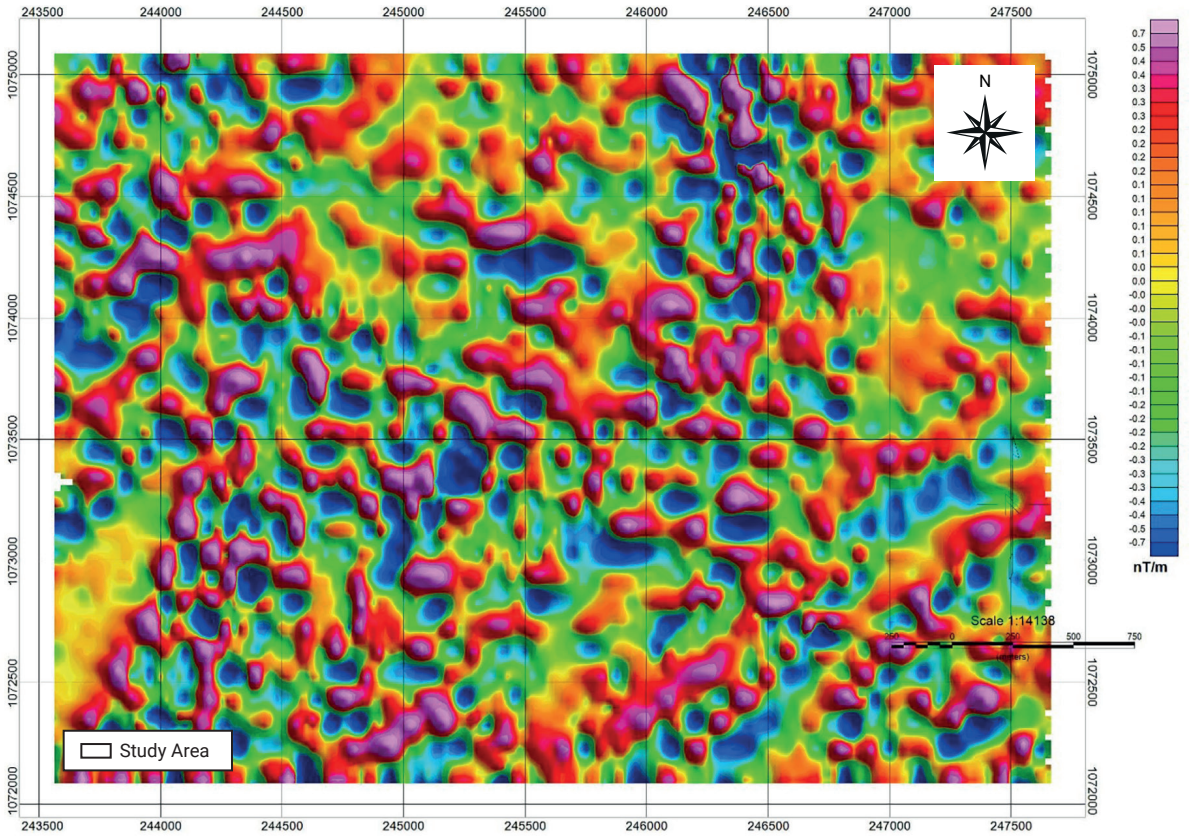

Figure 5. First Vertical Derivative map.

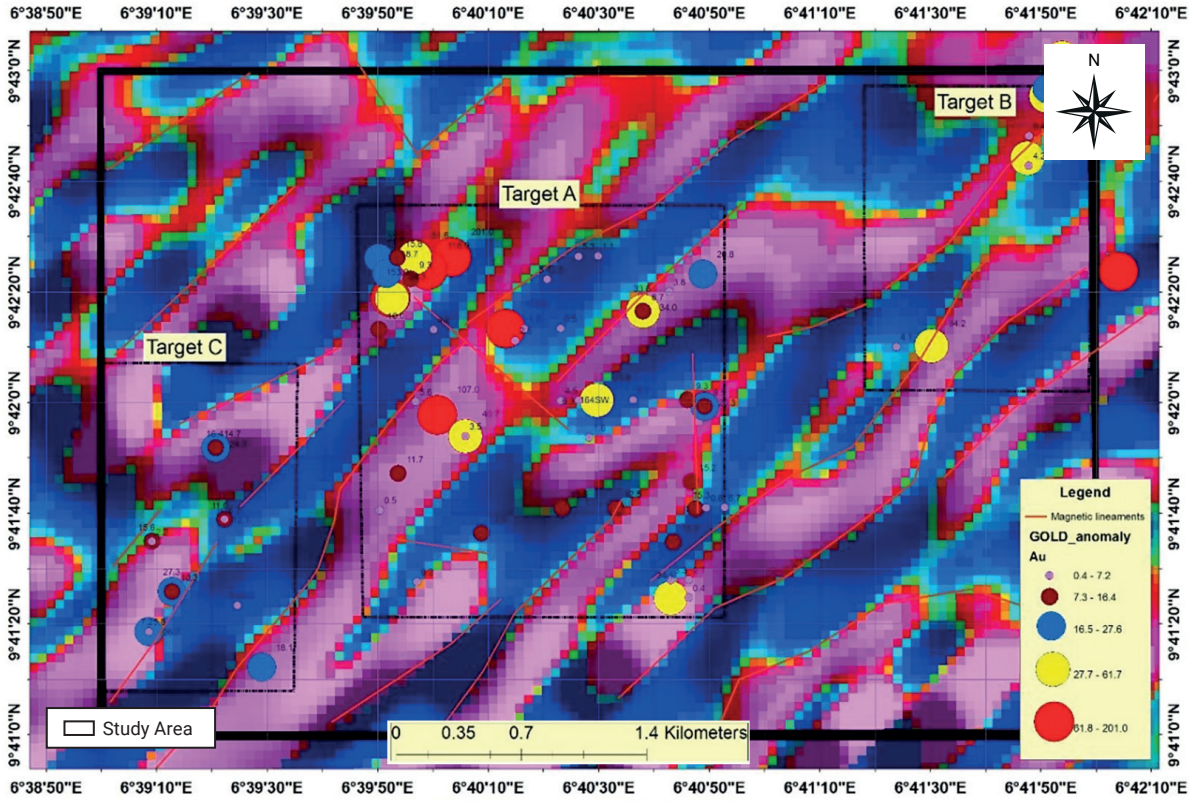

Figure 6. Second vertical derivative map showing the target areas and the magnetic lineaments.

picted with purple, brown, blue, yellow and red colours, in order of increasing magnetic intensity: 0.4-7.2, 7.3-14.4, 14.5-27.6, 27.7-41.7 and 41.8-201.0 respectively. The gold mineralization is found generally trending in the North – East direction.

4.1.5. Analytical Signal and Horizontal derivative

The analytical signal filter (Figure 7) was applied to determine the source positions of the magnetic anomaly irrespective of direction and remnant magnetization of the sources effect (Silva *et al.*, 2003). The high analytical signal amplitudes were correlated with the most significant concentrations of mineral deposits within Owu (Nabighian, 1972, Reeves *et al.*, 1998). Analytical signal map was useful in the location of edges of magnetic source bodies were remanence and (or) low magnetic latitude complicates interpretation (Thompson, 1982, Ademila *et al.*, 2019; Okpoli *et al.* 2022).

Figure 7a illustrate the structural network-faults of two pronounced orogenies which were clearly delineated. The contoured mineralized schist and other mineralized zones/alteration zones in the study area. The magnetic structures are highlighted with white broken lines. Figure 7b shows the horizontal gradient derivative map and the normalized derivative highlights locations of magnetic bodies within the survey area. Unlike the directional derivatives, it forms a positive response over a magnetic source body.

4.2. Induced Polarization

4.2.1 IP Interpretation

The induced polarisation data were acquired along the east-west direction (Fig.8). The survey lines were designed to cut across the strike, in view of measuring zones of high chargeability and apparent resistivity values.

The IP module of Oasis Montaj software was used in plotting IP chargeability and resistivity data pseudo sections. The resulting plots presents a vertical section showing the variation of IP chargeability and conductivity of materials at the subsurface along the survey profile. The pseudo section of some of the IP profiles are presented and briefly described below comprising both the IP chargeability plot and resistivity. The high IP chargeability portions are in pink, while the low IP areas are in green-blue. In the resistivity section, the low areas are in pink, while the blue areas are the high resistive area.

The pseudo-sections of high and low apparent chargeability and resistivity are illustrated in Figure 9 with the colour scale on

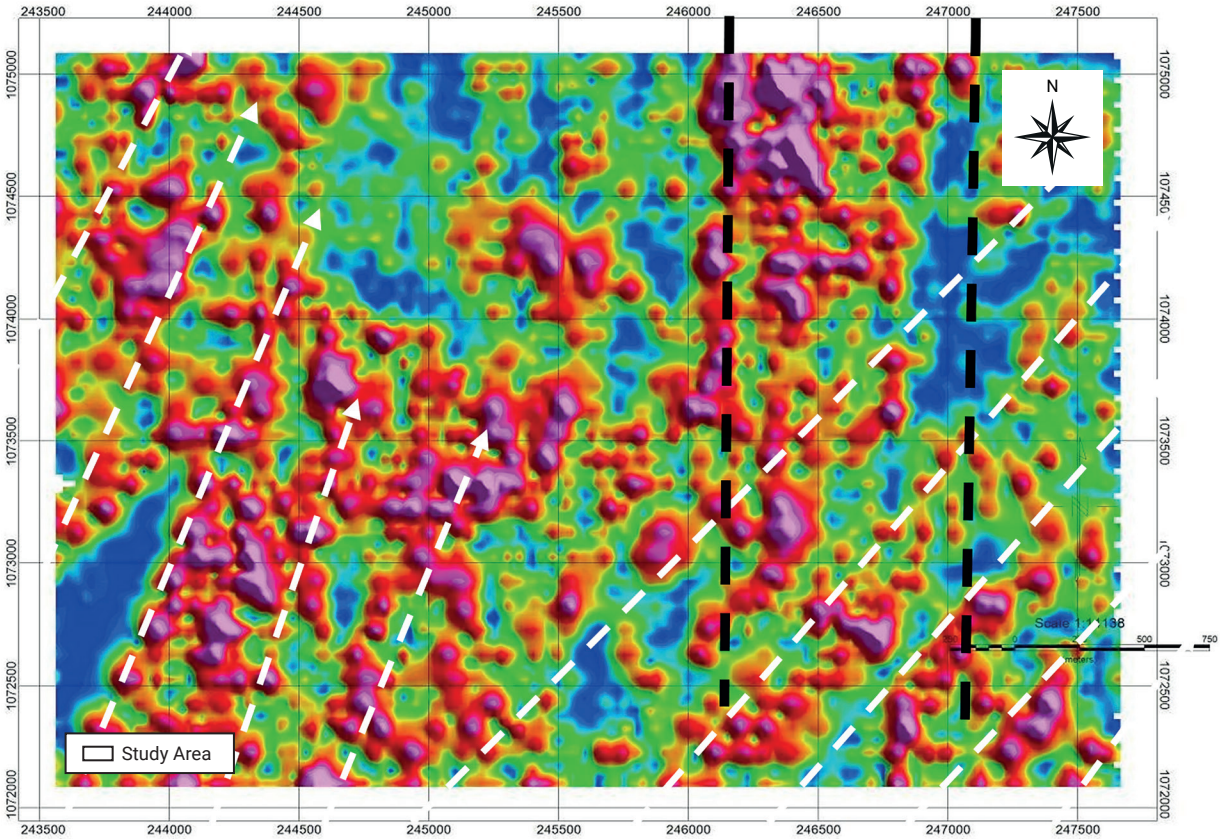

Figure 7a. Analytical signal map.

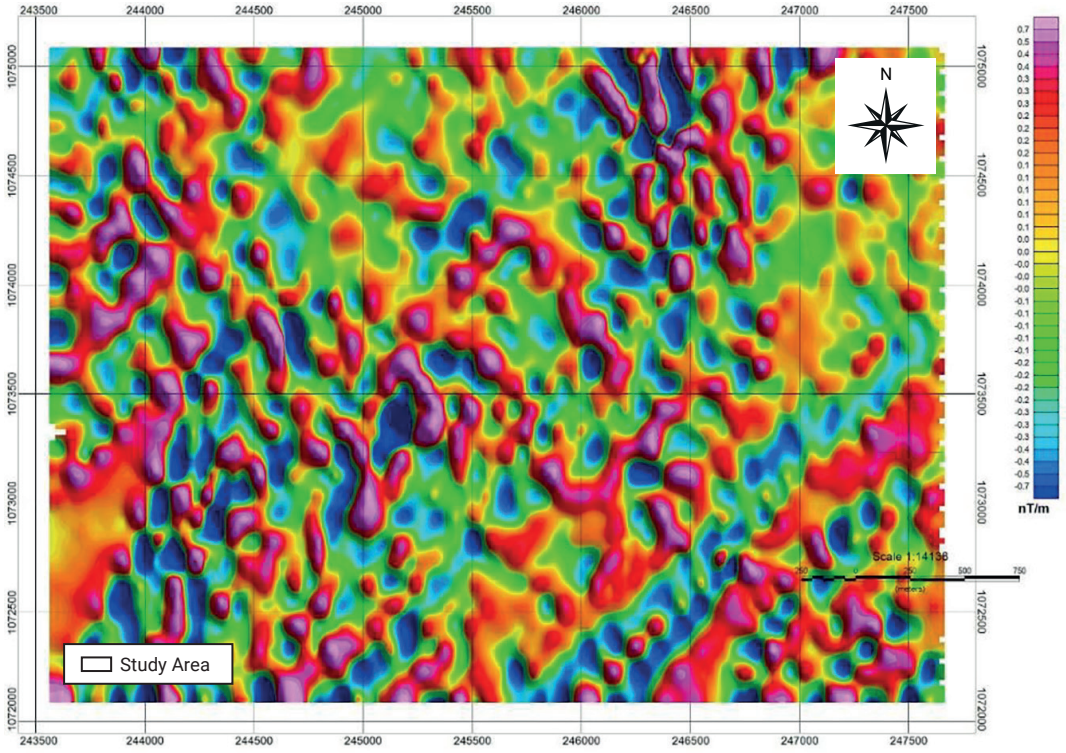

Figure 7b. Horizontal Gradient map.

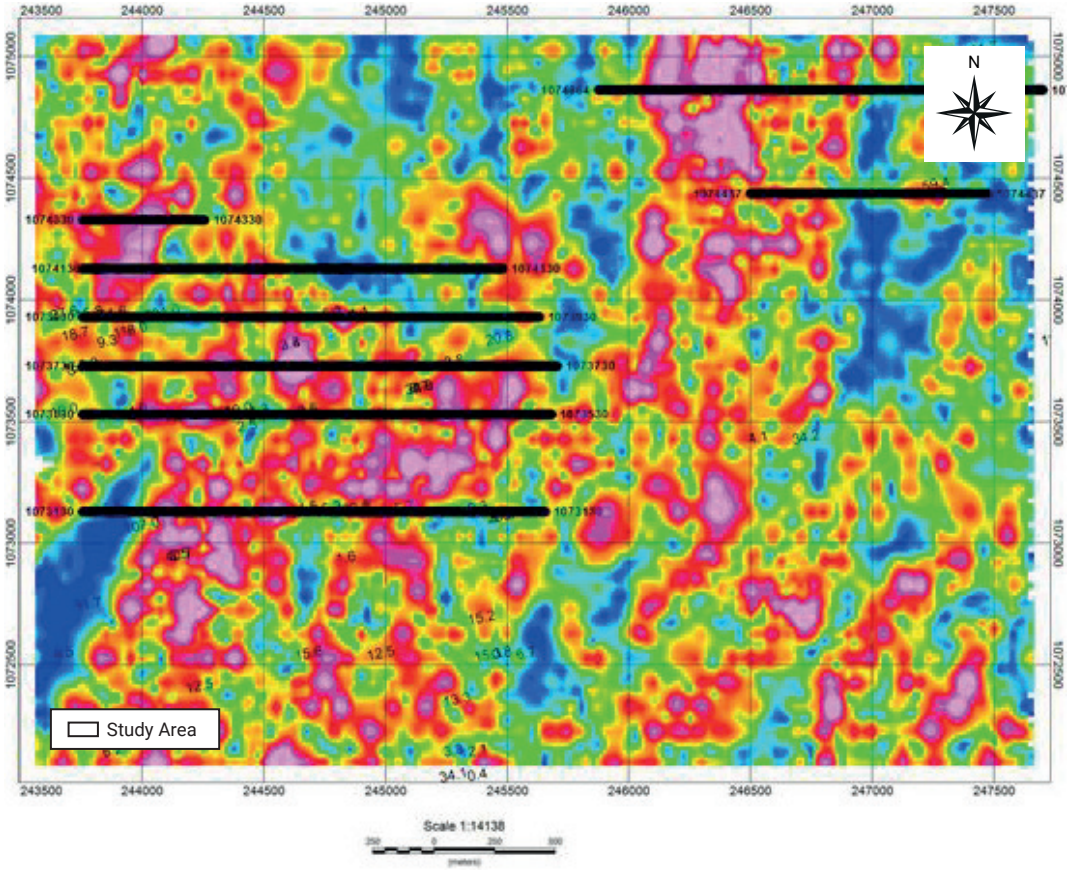

Figure 8. IP data acquired over the interpreted magnetic anomalies.

the side, where the pink zones indicate zones of high chargeability or resistivity and the blue zone shows areas of low chargeability and resistivity. The data plots were usually interpreted as high chargeability are related to conductive structures near the surface or at greater depth while apparent resistivity is due to high resistive units at or near the surface. Owed to the high disseminated nature of the ore body, it is more likely to have high resistivity correlated to high chargeability. Therefore, zones with both chargeability and high resisitivity or high chargeability and high resistive or high chargeability and resistive occurring close to each other were selected to delineate the anomaly causing zones to depth.

The pseudo section plot shows that the chargeable values are trending in the NE-SW direction around longitudes 243800E to 244200E. It seems to be another trend of chargeable values trending NW-SE from longitude 244500E intersecting the NE trending mineralization at 244200E. Moving East of the profile, with a seeming increase in resistivity, the pseudo-section plot of 1074437N shows a high resistive top layer that runs across the profile; this could be a sandy top layer. It also shows strong chargeability around longitudes 246500E to247000E. This could be localized mineralization.

The chargeable value on the eastern anomaly of pseudo-section at 1074864N (dipole-dipole array) is 40mV/V, where fire assay of pan soil concentrates detected up to 43 ppm of gold.

5. Conclusion

Geological mapping of the study area indicated that the mineralization pattern is structurally controlled and consistent with the dominant magnetic trend of NE-SW. Suspected anomalous sulphide concentration locations generally align with the magnetic inflection point, where magnetic bodies or lineaments are expected to be located at the subsurface.

Gold occurrences around the study area varies in distribution and potentials. Two modes of gold mineralization have been identified around the locality: Primary gold in the veins, associated with quartz veins that intruded the schist belt and sheared zones. Secondary gold mineralization concentrated by mechanical processes as alluvial deposits and occurring as placers and paleo-placers along stream channels or as eluvial deposit resulting from in-situ break down of gold bearing vein rocks to form considerable concentrations of gold-bearing gravely layer and saprolite above the bedrock.

The ground magnetic surveys and time domain induced polarisation documented the relationship between the gold anomalous locations and the North-east sheared zone traversing the centre of Owu. The primary gold-sulphide mineralisation suggested altered brecciated/ hydrothermally generated resource.

Conflicts of interest: The authors declare that there is no conflicts of interest in this original research paper in whatever form.

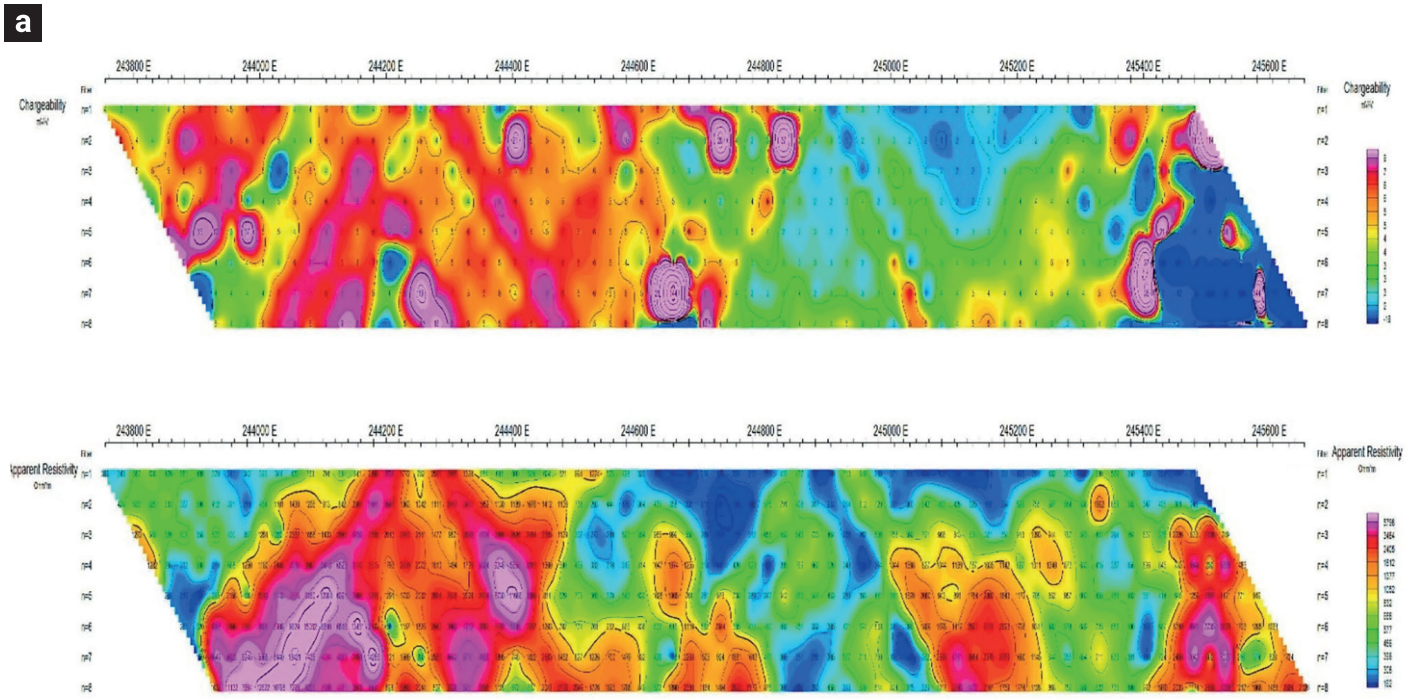

Figure9a. Pseudo section plot of 1073130N.

b

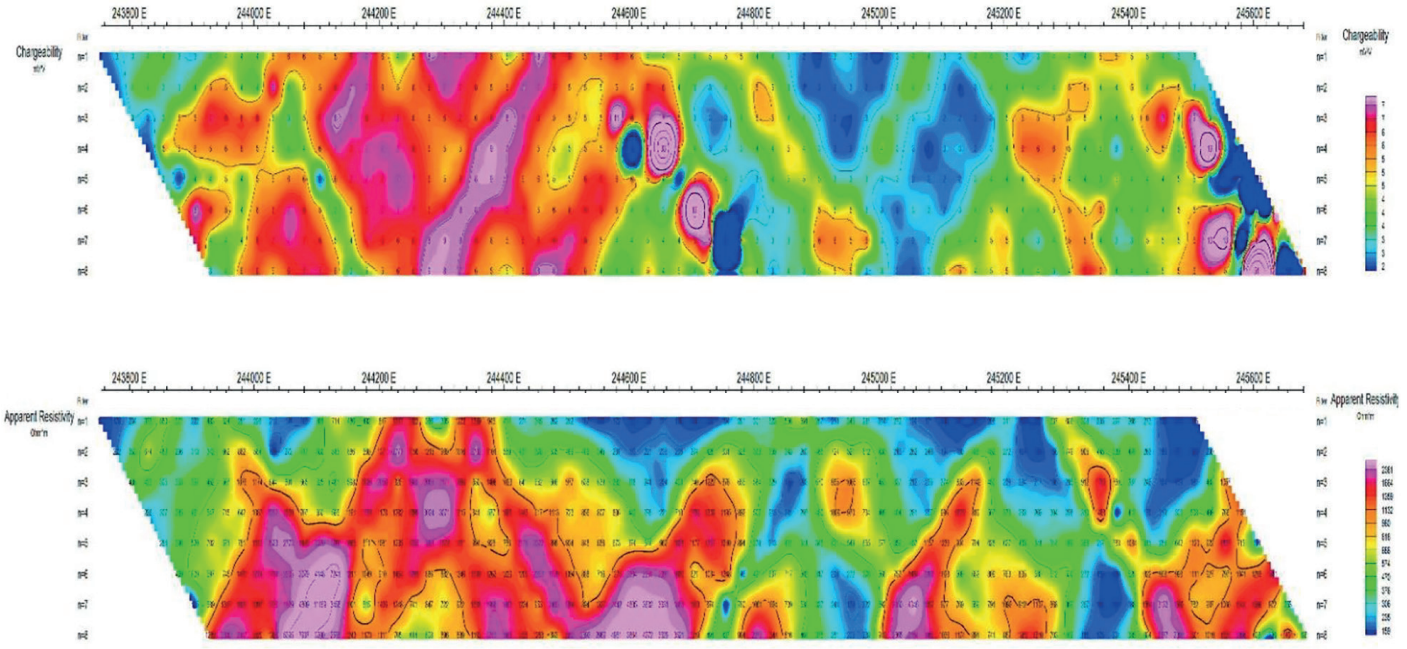

Figure9b. Pseudo section plot of 1073530N.

c

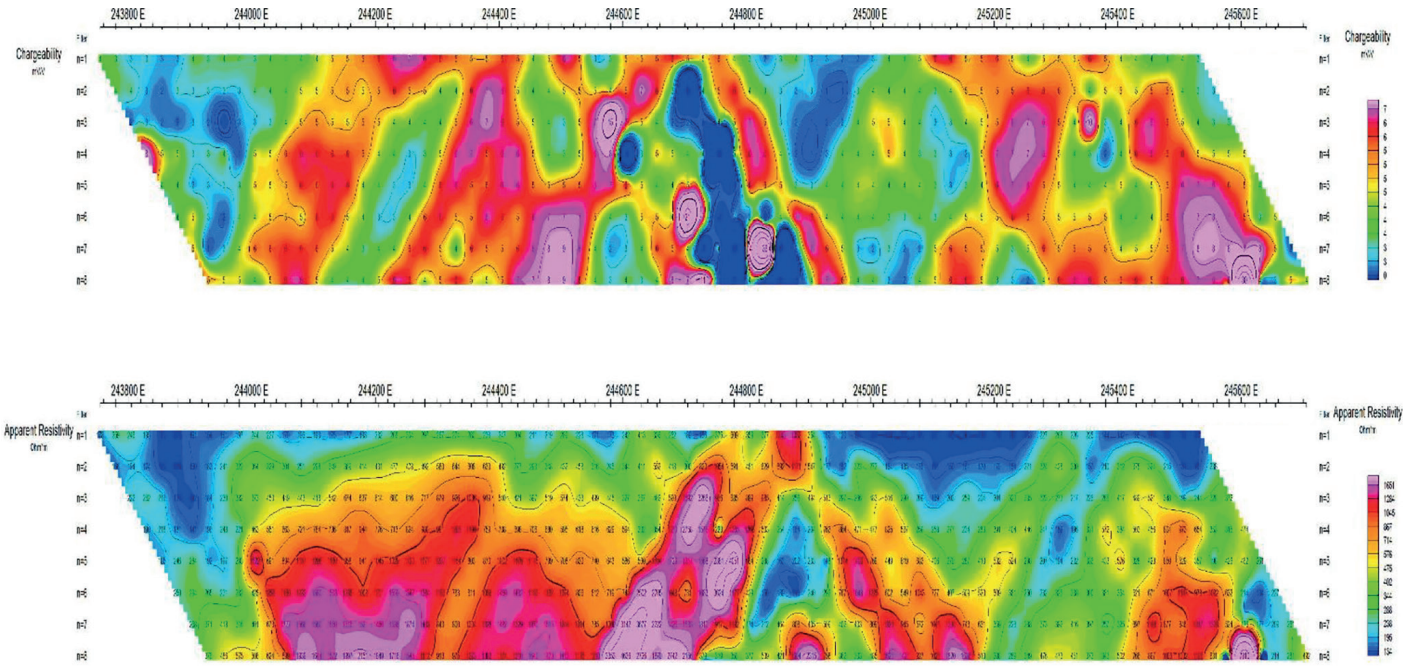

Figure9c. Pseudo section plot of 1073730N.

d

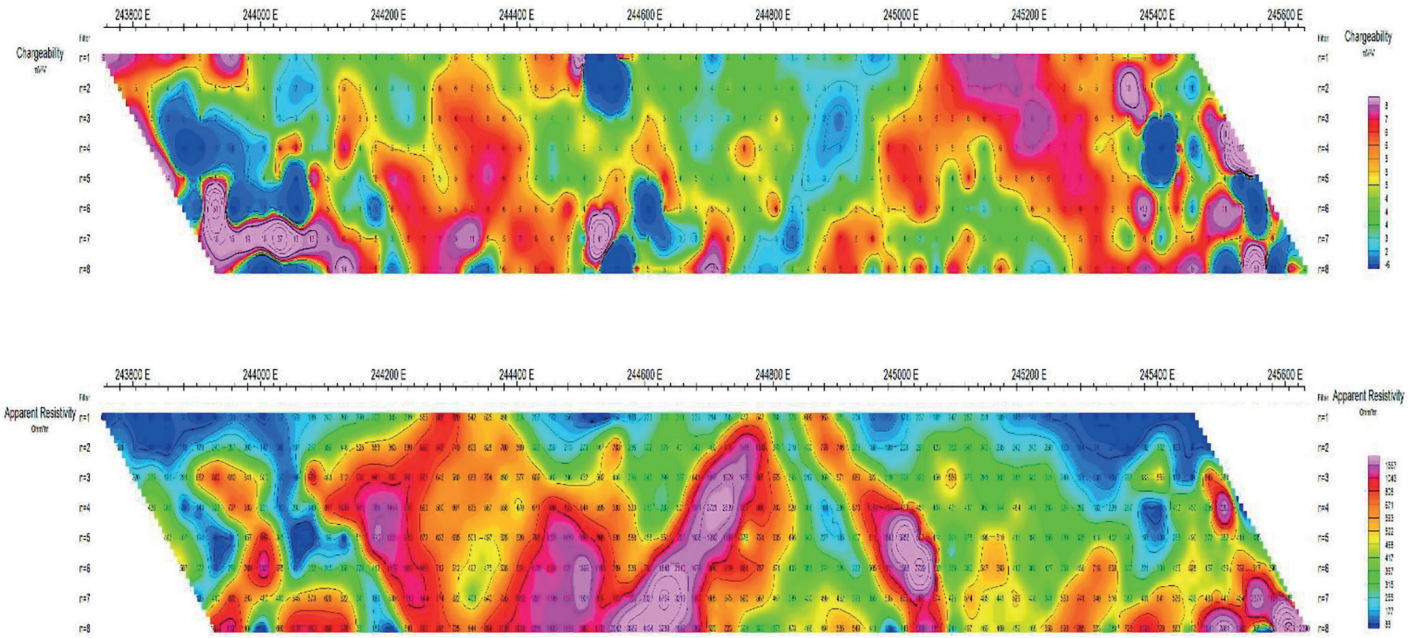

Figure9d. Pseudo section plot of 1073930N.

e

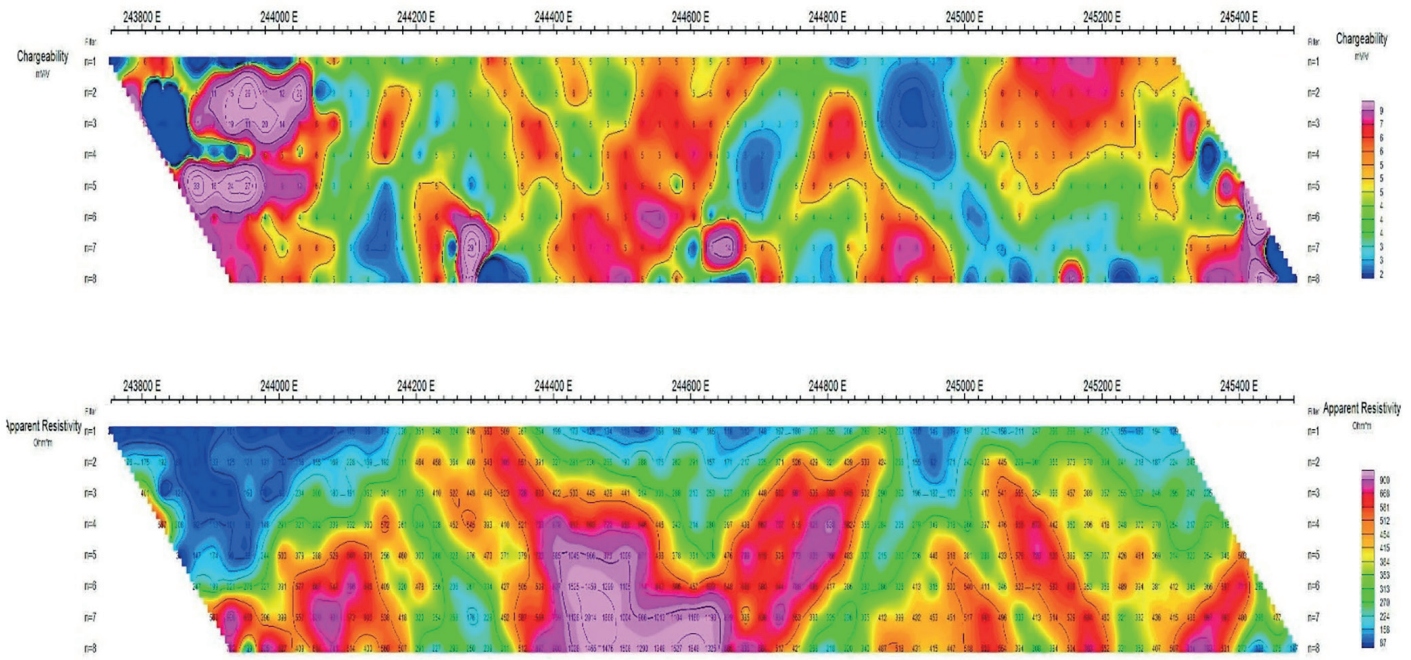

Figure 9e. Pseudo section plot of 1074130N.

f

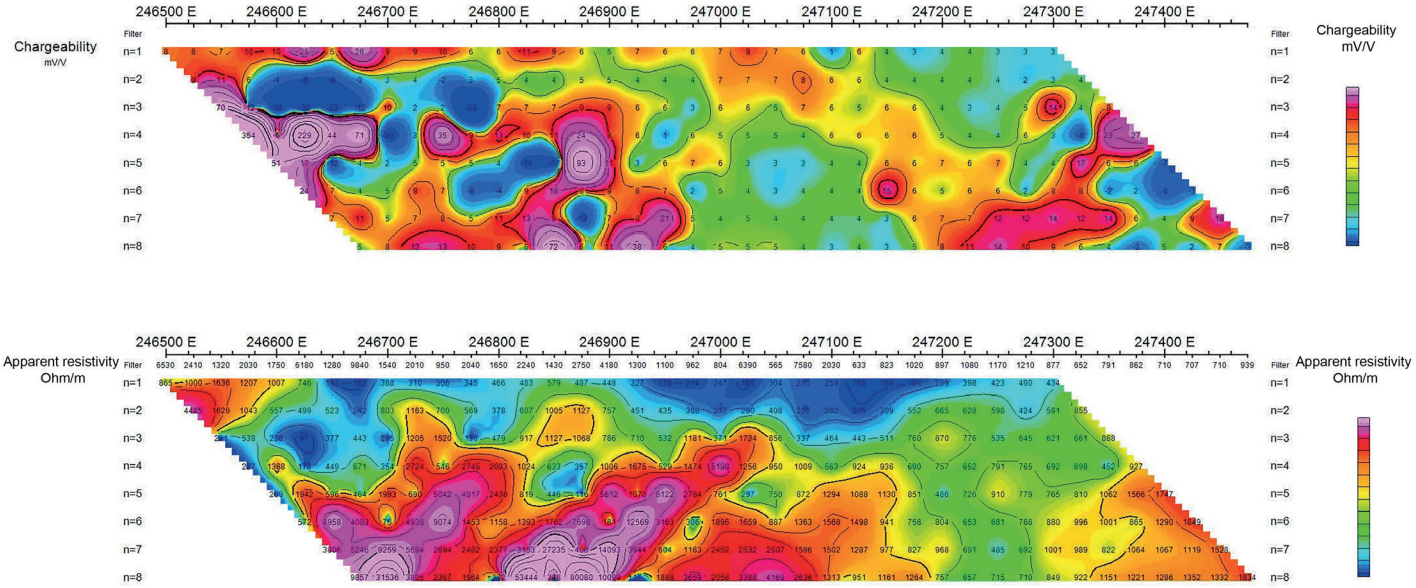

Figure9f. Pseudo section plot of 1074437N.

6. Acknowledgments

The authors would like to thank the Geodel integrated services for making the dataset available for academic purpose.

8. References

Ademila, O., Okpoli, C.C. & Ehinmitan, D. (2019). Geological and Lithological Mapping of Part of Igarra Schist Belt Using Integrated Geophysical Method. *Earth Sciences Pakistan*, 3(1):1-9.

Ajibade, A. C. (1988). *Structural and tectonic evolution of the Nigerian basement with special reference to NW Nigeria*. In International Conference on Proterozoic Geology Tectonics High-Grade Terrains (Ife, Nigeria).

Ekwueme, B.N.& Matheis, G. (1995). *Geochemistry and economic value of pegmatitesin the Precambrian basement of southeastern Nigeria* (Oxford & IBH Publishing Company, New Delhi).

Elueze, A.A. (1981). Geochemistry and petrotectonic setting of metasedimentary rocks of the schist belt of Ilesha area, Southwestern Nigeria. *J. Min. GEOL.* 19(1): 194-197.

Fitches, W.R., Ajibade, A.C., Egbuniwe, I.G., Holt, R.W. & Wright, J.B. (1985). Late Proterozoic Schist belts and Plutonism in NW Nigeria. *Jour. Of Geol. Soc.* London, 142, pp. 319-337.

Gunn, P., Maidment, D., & Milligan, P. (1997). Interpreting aeromagnetic data in areas of limited outcrop. *AGSO Journal of Australian Geology & Geophysics*, 17(2): 175-185.

Haruna, I.V. (2017). Review of the Basement Geology and Mineral Belts of Nigeria. IOSR *Journal of Applied Geology and Geophysics (IOSR-JAGG)*, Volume 5(1)P 37-45

Hilson, G. (2006). The socio-economic impacts of artisanal and small-scale mining in developing countries. Taylor & Francis.

Ho, S.E. & Groves, D.I. (1987). *Recent advances in understanding Precambrian gold deposits. Geology* Department and University Extension, University of Western Australia Publication.

Kerrich, R. & Wyman, D. (1990). Geodynamic setting of mesothermal gold deposits: an association with accretionary tectonic regimes. Geology, 18: 882-885.

Kuster, D. (1990). Rare-metal pegmatites of Wamba, Central Nigeria-their formation inrelation to late, Pan-African granites. *Mineralum Deposita* 25: 25-33.

Maurin, J.C. & Lancelot, J.R. (1990). Structural setting and U-Pb dating of Uranium Mineralization from the Northeastern part of Nigeria (Upper Benue Region). *Journal of African Earth Sciences*, 10:421-433

McCurry, P. & Wright, J.B. (1977). Geochemistry of calc-alkaline volcanics in northwestern Nigeria, and a possible Pan-African suture zone. *Earth Planet. Sci. Lett.* 37:90-96

McDonald, A.I. (1986). *An international symposium on the geology of gold.* Proceedings of gold '86. Toronto, pp. 517.

Milligan, P. & Gunn, P. (1997). Enhancement and presentation of airborne geophysical data. *AGSO Journal of Australian Geology & Geophysics*, 17(2):63-75.

Nabighian, M.N. (1972). The analytical signal of two-dimensional mag-

netic bodies with polygonal cross-section: Its properties and use for automated anomaly interpretation. *Geophysics*, 37:501-517.

Okpoli, C.C. (2013). "Sensitivity and Resolution Capacity of Electrode Configurations". International Journal of *Geophysics*, vol.2013, Article ID 608037, 12 pages, doi: **https://doi.org/10.1155/2013/608037**

Okpoli, C.C., Ogbole J.O., Oyeshomo, A. V. & Okanlawon, G.O (2022). Mineral exploration of Iwo-Apomu southwestern Nigeria using aeromagnetic and remote sensing. *Egyprian Journal of remote sensing and Space sciences*, 25: 371-385

Okpoli, C.C. & Akinbulejo B. (2021). Aeromagnetic and electrical resistivity mapping for groundwater development around Ilesha Schist Belt, osuthwestern Nigeria. Journal of Petroleum exploration and production technology. doi: **https://doi.org/10/1007/s13202-021-01307-x**

Reeves, C.V., Macnab, R. & Maschenkov (1998). Compiling all the world's magnetic anomalies, *EOS American Geophysical Union*, July 14, Pp. 338

Silva, A., Pires, A., McCafferty, A., De Morales, R. & Xia, H. (2003). Application of Airborne Geophysical Data to Mineral Exploration in the Uneven exposed Terrains of the Rio Das Velhas Greenstone Belt. *Revista Brasileira de Geociencias*, 33: 17-28

Thompson, D.T. (1982). "EULDPH-A new technique for making computer - assisted depth estimates from magnetic data", *Geophysics*, 47: 31-37.

Truswell, J.F. & Cope, R.N. (1963). The geology of parts of Niger and Zaria provinces, Northern Nigeria. *Bulletin No. 29.* Published by Geological Survey of Nigeria. pp.17-22.